RADC-TR-90-105
Final Technical Report
June 1990

NONLINEAR JOINT TRANSFORM PROCESSOR

University of Connecticut

Bahram Javidi

APPROVED FOR PUBLIC RELEASE; DISTRIBUTION UNLIMITED.

Rome Air Development Center
Air Force Systems Command
Griffiss Air Force Base, NY 13441-5700

This report has been reviewed by the RADC Public Affairs Division (PA) and is releasable to the National Technical Information Service (NTIS). At NTIS it will be releasable to the general public, including foreign nations.

RADC-TR-90-105 has been reviewed and is approved for publication.

APPROVED: Joseph L. Horner

JOSEPH L. HORNER
Project Engineer

APPROVED: Harold Roth

HAROLD ROTH
Director of Solid State Sciences

FOR THE COMMANDER: James W. Hyde III

JAMES W. HYDE III.
Directorate of Plans & Programs

If your address has changed or if you wish to be removed from the RADC mailing list, or if the addressee is no longer employed by your organization, please notify RADC (ESOP) Hanscom AFB MA 01731-5000. This will assist us in maintaining a current mailing list.

Do not return copies of this report unless contractual obligations or notices on a specific document require that it be returned.

REPORT DOCUMENTATION PAGE

Form Approved
OPM No. 0704-0188

1. AGENCY USE ONLY (Leave Blank)	2. REPORT DATE	3. REPORT TYPE AND DATES COVERED
	June 1990	Final Sep 88 to Aug 89

4. TITLE AND SUBTITLE
NONLINEAR JOINT TRANSFORM PROCESSOR

5. FUNDING NUMBERS
C - F30602-88-D-0025
PE - 62702F
PR - ILI6
TA - 11
WU - 10

6. AUTHOR(S)
Bahram Javidi

7. PERFORMING ORGANIZATION NAME(S) AND ADDRESS(ES)
University of Connecticut
Department of Electrical Engineering
Storrs, CT 06268

8. PERFORMING ORGANIZATION REPORT NUMBER
N/A

9. SPONSORING/MONITORING AGENCY NAME(S) AND ADDRESS(ES)
Rome Air Development Center (ESOP)
Hanscom AFB MA 01731-5000

10. SPONSORING/MONITORING AGENCY REPORT NUMBER
RADC-TR-90-105

11. SUPPLEMENTARY NOTES
RADC Project Engineer: Dr. Joseph L. Horner/ESOP/ (617) 377-3841

12a. DISTRIBUTION/AVAILABILITY STATEMENT
Approved for public release; distribution unlimited.

12b. DISTRIBUTION CODE

13. ABSTRACT (Maximum 200 words)

A nonlinear joint transform image correlator is investigated. The Fourier transform interference intensity is thresholded to provide higher correlation peak intensity and better defined correlation spot. Analytical expressions for the thresholded joint power spectrum is provided. The effects of the nonlinearity at the Fourier plane on the correlation signals at the output plane is investigated. The correlation signals are determined in terms of the nonlinear characteristics of the spatial light modulator (SLM) at the Fourier plane. We show that thresholding the interference intensity results in a sum of infinite harmonic terms. Each harmonic term is envelope modulated due to the nonlinear characteristics of the device, and phase modulated by m times the phase modulation of the nonthresholded joint power spectrum. The correct phase information about the correlation signal is recovered for the first order harmonic of the thresholded interference intensity. We show that various types

14. SUBJECT TERMS
Pattern Recognition, Information Processing, Target Detection, Optical Correlation, Joint Transform Optical Correlator, Nonlinear Joint Transform Processor

15. NUMBER OF PAGES
40

16. PRICE CODE

17. SECURITY CLASSIFICATION OF REPORT	18. SECURITY CLASSIFICATION OF THIS PAGE	19. SECURITY CLASSIFICATION OF ABSTRACT	20. LIMITATION OF ABSTRACT
UNCLASSIFIED	UNCLASSIFIED	UNCLASSIFIED	UL

19. Abstract (Continued).

of correlation signals can be produced simply by varying the severity of the nonlinearity and without the need to synthesize the specific matched filter. For example, a phase-only correlation signal is produced by selecting the appropriate nonlinearity.

Table of Contents

1. Introduction

We have investigated an optical system where the correlation between the images can be performed by nonlinear correlation[1-8] which has substantially superior performance compared to that of the classical optical correlator. This optical processor is joint Fourier transform correlator (JTC) based system[1] which allows both the input scene and the reference objects to be updated in real time. The nonlinear image correlator uses nonlinearity at the Fourier plane to threshold the Fourier transform interference intensity. The performance of the nonlinear optical correlator has been compared to that of the classical optical correlator in the areas of light efficiency,[9-12] correlation peak to sidelobe ratio, autocorrelation width, and cross–correlation sensitivity. It is shown that compared with the classical correlator, the bipolar joint transform correlator provides significantly higher peak intensity, larger peak to sidelobe ratio, narrower autocorrelation width, and better cross–correlation sensitivity. Since the autocorrelation functions have small width, larger reference images can be used, and the restriction on the locations of the images and their autocorrelation width, which exists for the classical joint transform correlator, is eliminated.

2. Joint Transform Correlation

In joint transform correlation,[1] the interference pattern intensity of the two signals located at the input plane is recorded. When the recorded intensity pattern is read out by a collimated beam, the correlation between the two signals can be obtained by taking the inverse Fourier transform of the recorded intensity pattern.

The reference pattern and the input pattern displayed on the monitor are imaged onto the spatial light modulator. The purpose of this spatial light modulator is to convert the incoherently diffused image of the monitor to a coherent image at the output of the device. For this reason, LCLV is called an image–to–image converter.

The coherent output image of the LCLV1 contains the input and the reference patterns displayed side by side. The Fourier transforms of the two patterns are obtained by the transform lens. The second spatial light modulator (LCLV2) is located at the Fourier plane of the transform lens. Thus, the input to LCLV2 is the interference between the Fourier transforms of the reference and the signal patterns.

The output image of the device is proportional to the intensity of the write–in signal. Therefore, the intensity of the interference between the Fourier transforms of two inputs is obtained at the device output. The inverse Fourier transform of the recorded intensity pattern is obtained by a second transform lens. The correlation between the two codes id displayed at the focal plane of the lens. The correlation intensity is detected by the detector array located at the output plane of the processor.

The operation of the joint transform correlator can be understood by considering a simple mathematical analysis of the system. The coherent output image of LCLV1 contains the reference and input patterns displayed side by side. The Fourier transforms of the two signals are taken by the transform lens. The second spatial light modulator (LCLV2) is located at the lens Fourier plane. Thus, the input to LCLV2 is:

$$f_1(\alpha,\beta) = F\{g(x,y)\} \exp(-i\frac{2\pi}{\lambda f}\alpha a) + F\{r(x,y)\} \exp(+\frac{2\pi}{\lambda f}\alpha a) \qquad (1)$$

where $g(x,y)$ is the output image function of the input signal, and $r(x,y)$ is the output image function of the reference signal, a is the distance of the signals from the optical axis, λ is the wavelength of the illuminating light, f is the focal length, and α is the spatial frequency coordinate.

The output image function of the signal $s(x,y)$ imaged onto the LCLV is:

$$g(x,y) = K_1 [s,(x,y)]^S \exp[i\, k_2 \log (\frac{s^2(x,y)}{I_0})], \qquad (2)$$

where K_1, and K_2 are constants, I_0 is a threshold value of illumination, and S is the slope of the intensity response curve.

A second LCLV (LCLV2) is used to record the intensity of the interference between the two Fourier transforms. Thus, the read–out light leaving LCLV2 becomes:

$$F_2(\alpha,\beta)= \left|F\{g(x,y)\} \exp(-\frac{2\pi}{\lambda f}\alpha a) + F\{r(x,y)\} \exp(+i\frac{2\pi}{\lambda f}\alpha a)\right|^2 \quad (3)$$

After some straightforward calculations, we have:

$$F_2(\alpha,\beta) = \left|F\{g(x,y)\}\right|^2 + \left|F\{r(x,y)\}\right|^2 + F\{g(x,y)\}\, F^*\{r(x,y)\} \exp(-\frac{i2\pi}{\lambda f}\alpha 2a)$$

$$+F^*\{g(x,y)\}\, F\{r(x,y)\} \exp(+\frac{i2\pi}{\lambda f}\alpha 2a) \quad (4)$$

By taking the inverse of the Fourier transform intensity, the output light distribution will contain the correlation between the input signal and the reference signal; i.e.,

$$f_3(x',y') = g_1(x',y') * g_1(x',y') + r(x',y') * r(x',y')$$

$$+r(x' - 2a,y') * g'(x',y') + r(x' + 2a,y') * g(x',y'), \quad (5)$$

where * denotes correlation. Thus, the light distribution at the output plane contains the correlation between the signals r(x,y) and g(x,y) displayed at (2a,0) and (-2a,0). The auto–correlations of r(x,y) and g(x,y) are displayed at the origin (0,0).

3. Nonlinear Optical Correlation

The nonlinear joint transform image correlator[1-8] can either use a Charge–Coupled Device (CCD) interfaced with a Spatial Light Modulator (SLM) or a high contrast optically addressed SLM at the Fourier plane. In the former case, the interference between the Fourier transforms of the reference and the input signals is produced by a Fourier transform lens, and the intensity distribution of the Fourier transform interference is obtained by a CCD array located at the fourier plane. The CCD array is connected to a thresholding network interfaced with a binary SLM, also at the Fourier plane, that reads out the binarized joint power spectrum in real time. A second transform lens is used to obtain the inverse Fourier transform of the thresholded interference intensity pattern, which can yield the desired correlation results. A high contrast optically addressed SLM can also be used at the Fourier plane to obtain the Fourier transform interference intensity and then threshold the interference intensity according to the nonlinear characteristics of the device.

In this section, we provide a mathematical analysis of the nonlinear joint transform image correlator. The effects of nonlinearity at the Fourier plane on the correlation signals at the output plane will be investigated. The correlation signals will be determined in terms of the nonlinear characteristics of the SLM at the Fourier plane. We investigate the effects of various types of nonlinear devices such as the k^{th} law nonlinearity and the hard clipping nonlinearity on the correlation signals. Analytical expressions for the thresholded joint power spectrum will be determined. The analysis provided here may be sued to study the effects of any arbitrary type of nonlinearity on the correlation signals. We show that the thresholded interference intensity can be considered as a sum of infinite harmonic terms. Each harmonic term is envelope modulated due to the nonlinear characteristics of the device, and phase modulated by m times the phase modulation of the nonthresholded joint power spectrum, where m is an integer. Thus, the correct phase information can be recovered for the first order harmonic term. The higher order correlation signals can be

removed by spatial filtering at the output plane. Various types of correlation signals such as the phase–only correlation signal can be produced by selecting the appropriate nonlinearity. Thus, the need to synthesize a specific matched filter to produce a specific correlation signal is eliminated. Computer simulations of the correlator are used to study the performance of the system and the results will be compared with those of the classical joint transform image correlator. We show that the nonlinear correlator can provide a much higher autocorrelation peak intensity, smaller autocorrelation sidelobes, narrower correlation width, and better discrimination sensitivity.

3.1 Analysis

In this section, we provide a mathematical expression for the correlation functions at the output plane of the nonlinear optical correlator. The thresholded interference intensity can be determined using the transform method of communication theory for the analysis of nonlinear devices.

The implementation of the nonlinear correlator using both high contrast optically addressed SLM and binary electrically addressed SLM is shown in Figure 1(a) and (b), respectively. Plane P_1 is the input plane that contains the reference signal and the input signal displayed on SLM_1. the incoherent images enter the input SLM and are converted to coherent images. The images are then Fourier transformed by lens FTL_1 and the interference between the Fourier transforms is produced at plane P_2. In Figure 1(a), the nonlinear joint transform image correlator is implemented using a high contrast optically addressed SLM at the Fourier plane. The Fourier transforms interference is displayed at the input of a high contrast optically addressed SLM to obtain the intensity of the Fourier transform interference. The high contrast optically addressed SLM can also threshold the joint power spectrum according to the nonlinear characteristics of the device. The thresholded interference intensity is read out from the output of SLM_2 by coherent light. The correlation signals can be produced at the output plane by taking the inverse Fourier

transform of the thresholded interference intensity distribution provided at the output of SLM_2. In Figure 1(b), an electrically addressed SLM is used to implement the nonlinear correlator. The intensity of the Fourier transform interference is obtained by a CCD array located at plane P_2 and is thresholded using a thresholding network. A SLM located at plane P_3 is used to read out the binarized intensity of the Fourier transform interference provided by the thresholding network. The correlation functions can be produced at plane P_4 by taking the inverse Fourier transform of the binarized interference intensity distribution at plane P_3.

The reference and input signals located at plane P_1 are denoted by $r(x+x_o,y)$ and $s(x-x_o,y)$, respectively. The light distribution at the back focal plane of the transform lens FTL_1 is the interference between the Fourier transforms of the two output image functions; i.e.

$$I(\alpha,\beta) = s(\alpha,\beta) \exp [i\varphi_S(\alpha,\beta)] \exp (-i\, x_o\alpha) + R(\alpha,\beta) \exp [i\varphi_R(m_{a',b}O] \exp (i\, x_o\alpha), \quad (6)$$

where (α,β) are the angular spatial frequency coordinates, and $S(\alpha,\beta) \exp [i\varphi_S(\alpha,\beta)]$ and $R(\alpha,\beta) \exp [i\varphi_R(\alpha,\beta)]$ correspond to the Fourier transforms of the input signals $s(x,y)$ and $r(x,y)$, respectively. Here, $R(\alpha,\beta)$ and $S(\alpha,\beta)$ are the amplitude spectrum and $\varphi_R(\alpha,\beta)$ and $\varphi_S(\alpha,\beta)$ are the phases of the Fourier transforms. The Fourier transform interference intensity distribution at plane P_2 can be written as:

$$E(\alpha,\beta) = |I(\alpha,\beta)|^2 = S^2(\alpha,\beta) + R^2(\alpha,\beta) +$$

$$S(\alpha,\beta) \exp [i\varphi_S(\alpha,\beta)]\, R(\alpha,\beta) \exp [-i\varphi_R(\alpha,\beta) \exp (-i\, 2x_o\alpha) +$$

$$S(\alpha,\beta) \exp[-i\varphi_S(\alpha,\beta)]\, R(\alpha,\beta) \exp [i\varphi_R(\alpha,\beta) \exp (i\, 2x_o\alpha) \quad (7)$$

In the classical case, the inverse Fourier transform of Equation (2) can produce the correlation signals at the output plane:

$$h(x',y') = R_{11}(x',y') + R_{22}(x',y') +$$

$$R_{12}(x'-2x_o,y') + R_{21}(x'+2x_o,y'), \tag{8}$$

where

$$R_{21}(x',y') = R_{12}(x',y') = \int\int s(\xi,\zeta)\, r(\xi-x',\zeta-y')d\xi d\zeta, \tag{9}$$

$$R_{11}(x',y') = \int\int s(\xi,\zeta)\, s(\xi-x',\zeta-y')d\xi d\zeta, \text{ and} \tag{10}$$

$$R_{22}(x',y') = \int\int r(\xi,\zeta)\, r(\xi-x',\zeta-y')d\xi d\zeta, \tag{11}$$

Here, the Fourier transform interference intensity provided by the CCD array is thresholded before the inverse Fourier transform operation is applied. The CCD array at the Fourier plane is connected to a binary SLM through a thresholding network so that the thresholded interference intensity distribution can be read out by coherent light.

The thresholded joint power spectrum can be considered as the output of a nonlinear system as shown in Figure 2. The nonlinear characteristics of the thresholding network is denoted by g(E) where E is the Fourier transforms interference intensity. An expression for the thresholded interference intensity can be obtained by a similar approach as the analysis of nonlinear systems using the transform method of communication theory. Let the Fourier transform of the nonlinear characteristic of the thresholding network be defined by:

$$G(\omega) = \int_{-\infty}^{\infty} g(E) \exp(-i\,\omega\, E)dE \tag{12}$$

The output of the nonlinear system is given by the inverse Fourier transform relationship, i.e.,

$$g(E) = \frac{1}{2\pi}\int_{-\infty}^{\infty} G(\omega) \exp(i\omega E)d\omega. \tag{13}$$

The thresholded interference intensity distribution can be obtained by substituting in Equation (5) for $E(\alpha,\beta)$ given by (2):

$$g(E) = \frac{1}{2\pi}\int_{-\infty}^{\infty} G(\omega) \exp(i\omega [R^2(\alpha,\beta) + S^2(\alpha,\beta)]$$

$$\exp\{i2\omega\, R(\alpha,\beta)\, S(\alpha,\beta) \cos[2x_o\alpha + \varphi_S(\alpha,\beta) - \varphi_R(\alpha,\beta)]d\omega \tag{14}$$

The second exponential factor can be expanded using the Jacobian–Anger formula:

$$\exp\{i2\omega\, R(\alpha,\beta)\, S(\alpha,\beta) \cos[2x_o\alpha - \varphi_R(\alpha,\beta) + \varphi_S(\alpha,\beta)] =$$

$$\sum_{v=0}^{\infty} \epsilon_v (i)^v J_v[2\omega\ R(\alpha,\beta)\ S(\alpha,\beta)]\ \cos[2vx_o\alpha + v\varphi_S(\alpha,\beta) - v\varphi_R(\alpha,\beta)] \tag{15}$$

where $\epsilon_v = \begin{cases} 1, & v=0 \\ 2, & v>0 \end{cases}$, and J_v is a Bessel function of the first kind, order v. Thus, the output of the nonlinear system is given by: (16)

$$g(E) = \sum_{v=0}^{\infty} \frac{\epsilon_v}{2\pi}(i)^v \int G(\omega) \exp\{i\omega[R^2(\alpha,\beta) +$$

$$S^2(\alpha,\beta)]\} J_v[2\omega R(\alpha,\beta)S(\alpha,\beta)] \cos[2vx_o\alpha + v\varphi_S(\alpha,\beta) - v\varphi_R(\alpha,\beta)]d\omega \quad (17)$$

The output of the thresholding network can be written as:

$$g(E) = \sum_{v=0}^{\infty} H_v [R(\alpha,\beta),S(\alpha,\beta)] \cos[2vx_o\alpha + v\varphi S(\alpha,\beta) - v\varphi_R(\alpha,\beta)] \quad (18)$$

where

$$H_v [R(\alpha,\beta),S(\alpha,\beta(] = \frac{\epsilon_v}{2\pi}(i)^v \int G(\omega) \exp\{i\omega[R^2(\alpha,\beta) +$$

$$S^2(\alpha,\beta)]\} J_v[2\omega R(\alpha,\beta)S(\alpha,\beta)]d\omega. \quad (19)$$

It can be seen from Equation (19) that for v=1, the nonlinear system has preserved the phase of the cross–correlation term $[\varphi_S(\alpha,\beta) - \varphi_R(\alpha,\beta)]$ and only the amplitude is affected. This explains the good correlation properties of the first order correlation signal at the output plane. The higher order terms in the series expansion [Equation 22] can be removed by spatial filtering at the output plane, although, the intensity of the higher order terms is relatively small compared with that of the first order correlation signal.

To investigate the effects of nonlinearity on the correlation signal, we consider two types of nonlinearity: the hard limiter and a general type k^{th} law device. The transfer characteristics of the limiter is shown in Figure 2. In the transform method of analysis, we consider the thresholding effects of the interference intensity on the terms corresponding to

the cross–correlation signals only. Thus. it is assumed that the unmodulated terms of Equation (15) have been subtracted from the joint power spectrum.

The Fourier transform of the full wave (odd) k^{th} law device is given by:

$$G(\omega) = \frac{2}{(i\omega)^{k+1}} \Gamma(k+2),\ K \leq 1, \tag{20}$$

where $\Gamma(\cdot)$ is the Gamma function, and K is the severity of the nonlinearity. $K=1$ corresponds to a linear device and $K=0$ corresponds to a hard clipping nonlinearity.

Substituting the Fourier transform of the nonlinearity in Equation 19, we have:

$$H_v\,[R(\alpha,\beta),S(\alpha,\beta)] = \Gamma(k+1)\,\frac{\epsilon_v}{\pi}\,(i)^{v-k-1}\int \frac{1}{\omega^{k+1}}\,J_v\,[2\omega R(\alpha,\beta)s(\alpha,\beta)]d\omega \tag{21}$$

Thus, $H_v[R(\alpha,\beta),S(\alpha,\beta)]$ can be written as:

$$H_v\,[R(\alpha,\beta),S(\alpha,\beta)] = 2\,\frac{\Gamma(k+1)\,\epsilon_v[2R(\alpha,\beta)S(\alpha,\beta)]^k}{2^{k+1}\Gamma(1-\frac{v-k}{2})\Gamma(1+\frac{v+k}{2})} \tag{22}$$

where $\Gamma(t)$ is the Gamma function.

The output of the nonlinearity using Equation (13) is given by:

$$g_k(E) = \sum_{\substack{v=1 \\ (v\ \text{odd})}}^{\infty} \frac{\epsilon_v\Gamma(k+1)[R(\alpha,\beta)S(\alpha,\beta)]^k}{2^K\Gamma(1-\frac{v-k}{2})\Gamma(1+\frac{v+k}{2})}\cos[2vx_o\alpha + v\varphi_S(\alpha,\beta) - v\varphi_R(\alpha,\beta)] \tag{23}$$

It can be seen from this equation that each harmonic term is phase modulated by v times the phase difference of the input signal and the reference signal Fourier transforms, and the higher order correlation signals are diffracted to $2vx_o$. The envelope of each

harmonic term is proportional to the k^{th} power of the product of the Fourier transform magnitudes of the input signal and the reference signal. If the phase of the input signal and the reference signal are the same, then the thresholded output will produce an output correlation signal corresponding to the inverse Fourier transform of the k^{th} power of the $2R(\alpha,\beta)S(\alpha,B)$. Furthermore, for $k=1$ the output will produce the linear correlation between the reference signal and the input signal.

The correct phase information of the joint power spectrum is obtained for the first order harmonic term ($v=1$) which yields:

$$g_{1\,k}(E) = \frac{2\Gamma(k+1)\left[R(\alpha,\beta)S(\alpha,\beta)\right]^{k}}{\Gamma\left(1-\frac{1-k}{2}\right)\Gamma\left(1+\frac{1+k}{2}\right)} \cos[2x_{o}\alpha + \varphi_{S}(\alpha,\beta) - \varphi_{R}(\alpha,\beta)]. \qquad (24)$$

If the input signal and the reference signal are the same, then Equation (24) will produce the thresholded joint power spectrum for autocorrelation signals; i.e.,

$$g_{1\,k}(E) = \frac{2\Gamma(k+1)}{\Gamma\left(1-\frac{1-k}{2}\right)\Gamma\left(1+\frac{1+k}{2}\right)}[R(\alpha,\beta)]^{2k}\cos[2x_{o}\alpha] \qquad (25)$$

It can be seen from Equation (25) that for $k=\frac{1}{2}$, the thresholded interference intensity will produce an autocorrelation signal that is identical to the autocorrelation signal obtained by a phase–only matched filter. Thus, a phase–only autocorrelation signal is produced without synthesizing a phase–only matched filter. Furthermore, various types of correlation signals can be produced simply by varying the degree of nonlinearity and without the need to synthesize the specific matched filter.

The effects of a hard clipped nonlinearity is determined by setting $k=0$ in Equation (25):

$$g_0(E) = \sum_{\substack{v=1 \\ (v \text{ odd})}}^{\infty} \frac{\epsilon_v}{\Gamma(1-\frac{v}{2})\Gamma(1+\frac{v}{2})} \cos[2vx_o\alpha + v\varphi_S(\alpha,\beta) - v\varphi_R(\alpha,\beta))]. \quad (26)$$

It can be seen from this equation that the amplitude modulation is entirely removed by the hard clipping operation. The correct phase of the joint power spectrum is obtained by the first order intermodulation term for v=1 which can be written as:

$$g_{1\,0}(E) = \frac{4}{\pi}\cos[2x_o a + \varphi_S(\alpha,\beta) - \varphi_R(\alpha,\beta)]. \quad (27)$$

If the Fourier phase of the input signal and the reference signal is the same, the output of the first order component is:

$$g_{1\,0}(E) = \frac{4}{\pi}\cos(2x_o\alpha) \quad (28)$$

Thus, the first order autocorrelation signal at the output plane is an impulse function with amplitude $\frac{2}{\pi}$ located at $2x_o$.

If a magneto–optic device (MOD) is used at the Fourier plane to read out the binarized interference intensity, then the transmittance function of the device will be the product of the thresholded interference intensity and the 2–D grating function of the device pixel structure. In this case, the light distribution at the output plane consists of the replicated correlation signals due to the sampling effects of the 2–D grating structure of the MOD. The intensity of the $(m,n)^{th}$ order spectra is weighted by $\text{sinc}^2 \frac{ma}{d} \text{sinc}^2 \frac{na}{d}$, where a is the pixel size, d is the period of the D–D grating structure of the device, and $\frac{a}{d}$ is the duty cycle of the grating. The intensities of the higher order spectra drop rapidly due to the large duty cycle of the device.

3.2 Computer Simulation Result

A numerical analysis of the nonlinear optical correlator is provided to study the thresholding effects of the transforms interference intensity on the correlation signals. To study the performance of the proposed system, we have used a 128×128 point 2–D fast Fourier transform (FFT) and the results are plotted using a 3–D plotting subroutine. The correlation tests are performed for the aerial image of a building. The first order autocorrelation term of the binary JTC for two input signals was produced. The Fourier spectrum $R^2(\alpha,\beta)$ was evaluated and the threshold value V_T of the interference intensity was determined. The Fourier component $g_{1a}(\alpha,\beta)$ that generates the first order autocorrelation signal was obtained. An inverse fast Fourier transform subroutine was used to obtain the first order autocorrelation signal.

In reference 8, we presented a computer simulation analysis of the nonlinear correlator to obtain the light distribution at the output of the processor by numerical techniques. In that numerical technique, the joint power spectrum was binarized to +1 and 0 according to a predetermined threshold value. An inverse FFT was then applied to obtain the correlation signals. Here, we have compared the first order autocorrelation term obtained by the Fourier series expansion technique and the first order autocorrelation term obtained by the numerical technique described in reference 8. The autocorrelation experiments are performed for characters F and F used as the input signals and the cross–correlation experiments are performed for the characters F and L used as the input signals. Table I illustrates the correlation results obtained by the Fourier series expansion technique. The results are compared to the correlation signals produced by the numerical technique which is obtained by taking the inverse FFT of the binarized Fourier transforms interference intensity (see reference 8). In this table, R_o^2 is the autocorrelation peak intensity, $R_o^2/S.L.^2$ is the ratio of the autocorrelation peak intensity to the maximum

Table I. Comparison between the nonlinear correlation results obtained by the Fourier series expansion technique and the results obtained by the numerical technique.[8]

	R_o^2	R_o^2/SL^2	FWHM (x'-y')	R_o^2/R_c^2
Correlation results obtained by binarizing the joint power spectrum	1.	11.5	(1-1)	14.2
Correlation results obtained by the Fourier series expansion techniques	1.13	8.82	(1-1)	11.94

*R_o^2 is the normalized first order autocorrelation peak intensity, SL^2 is the largest sidelobe intensity, and $FWHM^2$ is the full correlation width at the half maximum. R_c^2 is the maximum cross–correlation intensity.

sidelobe intensity, and FWHM is the full correlation width at half maximum. The correlation intensities are normalized by the peak intensity of the results obtained by the numerical technique. R_c^2 is the maximum cross–correlation intensity.

The results indicate (See Table I) that the correlation signals obtained by these methods are almost equivalent and have the same autocorrelation width, 13% difference in the auto–correlation peak intensity, and 7% difference in the autocorrelation peak to sidelobe ratio, and 15% difference in the ratio of autocorrelation peak to the maximum cross–correlation intensity. Thus, the Fourier series expansion technique represents a reasonable accurate description of the first order Fourier component.

We have also investigated the thresholding effects of a k^{th} law nonlinearity on the Fourier transforms interference intensity. This case corresponds to using a nonlinearity at

the Fourier plane that has an input/output characteristics of a k^{th} law device. Equation (24) is used to generate the correlation signals for various degrees of nonlinearity. The correlation results obtained by binarized joint power spectrum[10] corresponds to using a hard clipping nonlinearity width k=0.

Figure 3(a) illustrates the modified Fourier transforms interference intensity where only the modulated terms are retained. The thresholded interference intensity distribution when a k^{th} law nonlinearity is used is shown in Figures 3(b) – (d). The nonlinearities correspond to k=0.9, 0.7, and 0.5 as shown in the figure. It can be seen from this figure that as the severity of nonlinearity increases the pixel values of the higher spatial frequencies of the interference intensity values of the higher spatial frequencies of the interference intensity increase. For a hard clipping nonlinearity, the amplitude modulation is entirely removed and only the phase information is retained.

The correlation signals for the input aerial image are shown in Figure 4. Figure 4(a) shows the correlation results when the interference intensity is not thresholded (k=1), and figure (b), (c), and (d) show the correlation results when the interference intensity is thresholded according to Equation (24) for k=0.9, 0.7, and 0.5. It is evident from this figure that the correlation signals corresponding to the thresholded interference intensity have higher peak intensities, higher peak to sidelobe ratios, and narrower correlation widths.

Table II illustrates the results of the tests for the linear and nonlinear correlation. In this table, R_o^2 is the autocorrelation peak intensity, $R_o^2/S.L.^2$ is the ratio of the autocorrelation peak intensity to the maximum sidelobe intensity, and FWHM is the full correlation width at half maximum. FWHM is determined by evaluating the points where the correlation intensity drops to one–half of its peak value. K is the degree of the nonlinearity for the k^{th} law device given by Equation (20).

Table II. Correlation results*

Correlator	k	R_o^2	$R_o^2/S.L.^2$	FWHM (x′-y′)
Linear Correlator	1	1	1.25	(35-41)
Nonlinear Correlator	0.9	1.86	1.53	(23-23)
Nonlinear Correlator	0.8	4.48	2.2	(5-7)
Nonlinear Correlator	0.7	15.3	4.14	(3-3)
Nonlinear Correlator	0.6	77.5	9.5	(1-1)
Nonlinear Correlator	0.5	559.	12.7	(1-1)

*R_o^2 is the first order autocorrelation peak intensity. $S.L.^2$ is the largest sidelobe intensity. k is the degree of nonlinearity. FWHM is the full correlation width at the half maximum.

It can be seen from this table that thresholding the interference intensity has significantly increased the autocorrelation peak intensity compared to the classical case. The linear correlator has a correlation peak intensity of unity, whereas the nonlinear correlator has a peak value of 1.86, 15.3, and 559 for k=0.9, 0.7, and 0.5, respectively. Consequently, if we have a correlator set up with a given laser source, using the nonlinear technique for k=0.5, an increase of 559 in the detector output voltage can be expected. Thresholding the interference intensity has also reduced the correlation sidelobes considerably for the nonlinear case. The linear correlator has a peak intensity to sidelobe intensity ratio of 1.25, whereas the nonlinear correlator has a peak to sidelobe ratio of 1.5, 4.1, and 12.7 for k=0.9, 0.7, and 0.5, respectively.

It is evident from Table II that thresholding the interference intensity has resulted in a significant reduction in the autocorrelation width and has produced impulse like autocorrelation functions for small k. The linear correlator has width of 35×41 pixels in the x′-y′ direction, whereas the nonlinear correlator has a width of 1×1 pixels in the x′-y′ direction for k=0.5.

We made some attempts to reduce the correlation width of the classical joint Fourier transform correlator by edge enhancement of the input signals. This results in a correlation width of 12×12 pixels in the x'-y' direction, no significant change in the size of the sidelobes, and 5.8 times decrease in the correlation peak intensity. Thus, the autocorrelation width obtained by binarization of the interference intensity is considerably better than the edge enhanced classical correlation results.

Multiple diffracted correlation terms are produced due to the thresholding of the Fourier transforms' interference intensity. However, the size of the higher orders appear small when compared to the first order diffracted correlation term. According to the computer simulations, the first order autocorrelation peak intensity is 15 times larger than the second order correlation peak intensity for k=0. Thus, the higher order correlation signals are much smaller than the first order correlation signal.

4. Conclusion

We have introduced a nonlinear image correlator with substantially superior performance compared to that of the classical optical correlator. This optical processor is joint Fourier transform correlator (JTC) based system which allows both the input scene and the reference objects to be updated in real time. The nonlinear image correlator uses nonlinearity at the Fourier plane to threshold the Fourier transform interference intensity. The performance of the nonlinear optical correlator has been compared to that of the classical optical correlator in the areas of light efficiency, correlation peak ot sidelobe ratio, autocorrelation width, and cross–correlation sensitivity. It was shown that compared with the classical correlator, the bipolar joint transform correlator provides significantly higher peak intensity, larger peak to sidelobe ratio, narrower autocorrelation width, and better cross–correlation sensitivity. Since the autocorrelation functions have small width, larger reference images can be used, and the restriction on the locations of the images and their

autocorrelation width, which exists for the classical joint transform correlator, is eliminated.

References

1. C.S. Weaver and J.W. Goodman, A technique for optically convolving two functions, Appl. Opt. 5 (1966), pp. 1248–1249.

2. Industrial Applications of Real–Time Signal Processing, edited by B. Javidi, SPIE Publications, Vol. 960, 1988.

3. B. Javidi, "Single Modulator Optical Correlator Architectures", to appear in the Journal of Applied Optics (1989).

4. B. Javidi et. al., "Image Deconvolution by Joint Transform Correlation", to appear in the Journal of Optics Communications (1989).

5. B. Javidi, "Programmable Optical Processor for Associative Retrieval", Journal of Optical Engineering, Vol. 28, No. 5, May 1989.

6. B. Javidi, "Analysis of Nonlinear Correlator, Proc. SPIE, Vol. 977, August 1988.

7. B. Javidi et. al., "Multiple Image Detection by Nonlinear Optical Correlation," Journal of Optical Engineering, Vol. 27, No. 4, April 1988.

8. B. Javidi et. al., ""Joint Transform Image Correlation Using a Binary Spatial Light Modulator at the Fourier Plane," Journal of Applied Optics, Vol. 27, No. 5, March 1, 1988.

9. H. John Caulfield, "Role of the Horner efficiency in the optimization of spatial filters for optical pattern recognition," Appl. Opt. 21, 4391, 1988.

10. J.L. Horner and H.O. Bartelt, "Two–bit correlation," Appl. Opt., Vol. 24, p. 2889, 1985.

11. D. Psaltis, E.G. Paek, S.S. Venkatesh, "Optical image correlation with a binary spatial light modulator," Opt. Eng., Vol. 23, p. 698, 1984.

12. D. Flannery et. al., "Application of binary phase–only correlation to machine vision," Opt. Eng. 27, 309, 1988.

6. Patents

B. Javidi, patent, "Joint Transform Image Correlation Using a Binary Spatial Light Modulator at the Fourier Plane," pending.

J.L. Horner and B. Javidi, patent, "Single Spatial Light Modulator Joint Transform Correlator," pending.

7. Involvement in Conferences, Workshops and Journals

Chairman of the conference, "Optical Information Processing", International Symposium on Optical and Optoelectronic Applied Science and Engineering, San Diego, California, August 1989.

Chairman of the conference, "Critical Review of Technology on Real–Time Optical Signal Processing," SPIE sponsored conference, International Symposium on Optical Engineering and Industrial Sensing, Detroit, Michigan, June 1988.

Chairman of the session, "Pattern Recognition," International Symposium on Optical Engineering and Industrial Sensing, Detroit, Michigan, June 1988.

Workshop on Optical Signal Processing, SPIE Meeting, International Symposium on Optical Engineering and Industrial Sensing, Detroit, Michigan, June 1988.

Guest editor of the May 1989 special issue of Optical Engineering on Optical Signal Processing.

Guest of editor of the April 1988 special issue of Optical Engineering on Optical Signal Processing.

8. Books and Refereed Journal Papers

Industrial Applications of Real–Time Signal Processing, edited by B. Javidi, SPIE publications, 1988.

B. Javidi et. al., "Single Modulator Optical Correlator Architectures", to appear in the Journal of Applied Optics, February 15, 1989.

B. Javidi et. al., "Image Deconvolution by Joint Transform Correlation:", to appear in the Journal of Optics Communications.

B. Javidi et. al., "Programmable Optical Processor for Associative Retrieval", Journal of Optical Engineering, Vol. 28, No. 5, May 1989.

B. Javidi and J.L. Horner, "Single SLM Optical Correlator," to appear in the Journal of Applied Optics, March 1989.

B. Javidi et. al., "Correlation Signal Recovery From an Undersampled Hologram," to appear in the Journal of Optical Engineering.

B. Javidi et. al., "Multiple Image Detection by Nonlinear Optical Correlation," Journal of Optical Engineering, vol. 27, No. 4, April 1988.

B. Javidi et. al., "Joint Transform Image Correlation Using a Binary Spatial Light Modulator at the Fourier Plane," Journal of Applied Optics, Vol. 27, No. 5, March 1, 1988.

B. Javidi et. al., "Nonlinear Optical Correlation," to appear in Applied Optics.

B. Javidi et. al., "Color Object Identification by Monochromatic Binary Correlation," Journal of Applied Optics, Vol. 27, No. 6, March 15, 1988.

B. Javidi et. al., "Rotation and Scale Sensitivity of a Binary Phase–Only Filter," Journal of Optic Communication, Vol. 65, No. 4, February 1988.

B. Javidi "Real–Time Joint Transform Image Correlation by Partially Coherent Read–Out Illumination," Journal of Applied Optics, Vol. 26, No. 18, September 1987.

9. Conference Proceedings (International and National Meetings)

B. Javidi, "Analysis of Nonlinear Optical Correlation", presented at the 1988 Optical Society of America Annual Meeting in Santa Clara, California, Journal of Optical Society of America, Vol. 6, No. 12, 1988.

B. Javidi et. al., "Single SLM Optical Pattern Recognition", presented at the 1988 Optical Society of America Annual Meeting in Santa Clara, California, Journal of Optical Society of America, Vol. 5, No. 12, 1988.

B. Javidi et. al., "Real–Time Deconvolution by Nonlinear Image Processing", presented at the 1988 Optical Society of America Annual Meeting in Santa Clara California, Journal of Optical Society of America, Vol. 5, No. 12, 1988.

B. Javidi et. al., "Synthetic Discriminant Function Based Nonlinear Correlation", presented at the 1988 Optical society of America Annual Meeting in Santa Clara, California, Journal of Optical Society of America, Vol. 5, No. 12, 1988.

B. Javidi et. al., "Single Spatial Light Modulator Joint Transform Correlator", Proceedings of SPIE on Optical Pattern Recognition, Vol. 1014, Symposium on Innovative Science and Technology, Los Angeles, California, January 1989.

B. Javidi et. al., "Nonlinear Optical Correlation of Multiple Targets by Synthetic Discriminant Function", Proceedings of SPIE on Optical Pattern Recognition, Vol. 1014, Symposium on Innovative Science and Technology, Los Angeles, California, January 1989.

B. Javidi, "A New Class of Nonlinear Optical Processors", The International Congress on Optical Science and Technology, Paris, France, April 1989.

B. Javidi, "Rotation Invariant Pattern Recognition by Nonlinear Signal Detection", The International Congress on Optical Science and Technology, Paris, France, April 1989.

B. Javidi, "Bipolar Nonlinear Correlator," Proceedings of the SPIE on Real–Time Signal Processing, Vol. 977,. San Diego, August 1988.

B. Javidi et. al., "Optical Associative Memory," Proceedings of the SPIE meeting on Real–Time Signal Processing, Vol. 977, San Diego, August 1988.

B. Javidi et al., "Programmable Optical Associative Memory," SPIE Conference on Real–Time Signal Processing, International Symposium on Optical Engineering and Industrial Sensing, Vol. 960, Detroit, Michigan, June 1988.

B. Javidi et. al., "Image Recognition and Classification by Code Division Multiplexed Hybrid Optical Processing," SPIE Conference on Real–Time Signal Processing, International Symposium on Optical Engineering and Industrial Sensing, Vol. 960, Detroit, Michigan, June 1988.

B. Javidi et. al., ""Multiple Image Recognition by Nonlinear Optical Correlation," SPIE Conference on Real–Time Signal Processing, Vol. 960, International Symposium on Optical Engineering and Industrial Sensing, Detroit, Michigan, June 1988 .

B. Javidi et. al., "Large Capacity Phase–Only Encoded Smart Correlators," SPIE Conference on Piece Recognition and Image Processing, International Symposium on Optical Engineering and Industrial Sensing, Vol. 956, Detroit, Michigan, June 1988.

B. Javidi et. al., "Code Division Multiplexed Generalized Phase–Only Encoded Filters," SPIE Conference on Piece Recognition and Image Processing, International Symposium on Optical Engineering and Industrial Sensing, Vol. 956, Detroit, Michigan, June 1988.

B. Javidi et. al., "Performance of a Bipolar Nonlinear correlator," SPIE Conference on Piece Recognition and Image Processing, International Symposium on Optical Engineering and Industrial Sensing, Vol. 956, Detroit, Michigan, June 1988.

B. Javidi, "Real–Time Object Recognition and Classification by Code Division Multiplexed Filters," Optical Society of America Meeting on Spatial Light Modulators, Lake Tahoe, Nevada, June 1988.

B. Javidi et. al., "Noise Performance of Nonlinear Optical Correlators," Optical Society of America Meeting on Spatial Light Modulators and Applications, Lake Tahoe, Nevada, June 1988.

B. Javidi, "Detection of Frequency Hopped Spread Spectrum Signals by Optical Computing", Advances in Optical Information Processing," Vol. 936, Orlando, Florida, April 1988.

B. Javidi, "Multi–channel Programmable Acousto–Optic Correlator," Proceedings of SPIE, Advances in Optical Information Processing III, Vol. 936, Orlando, Florida, April 1988.

B. Javidi et. al., "Comparison of Bipolar Joint Transform Image Correlators and Phase–Only Matched Filter Correlators," Proceedings of the SPIE, Digital and Optical Shape Representation and Pattern Recognition, Vol. 938, Orlando, Florida, April 1988.

B. Javidi et. al., "Space–variant Image Correlation Using an Electrically Addressed Spatial Light Modulator at the Fourier Plane," Proceedings of SPIE, Digital and Optical Shape Representation and Pattern Recognition, Vol. 938, Orlando, Florida, April 1988.

B. Javidi, "Frequency Hopped Spread Spectrum Optical Processor," presented at the 1987 Optical Society of America Annual Meeting in Rochester, New York, Journal of Optical Society of America, Vol. 4, No. 13, 1987.

B. Javidi, "Real–Time Joint Transform Correlation by Partially Coherent Read–Out Illumination," presented at the 1987 Optical Society of America Annual Meeting in Rochester, New York, Journal of Optical Society of America, Vol. 4, No. 13, 1987.

B. Javidi, "Multiple Image Recognition by Code Division Multiplexed Phase–Only Filters," presented at the 1987 Optical Society of America Annual Meeting in Rochester, New York, Journal of Optical Society of America, Vol. 4, No. 13, 1987.

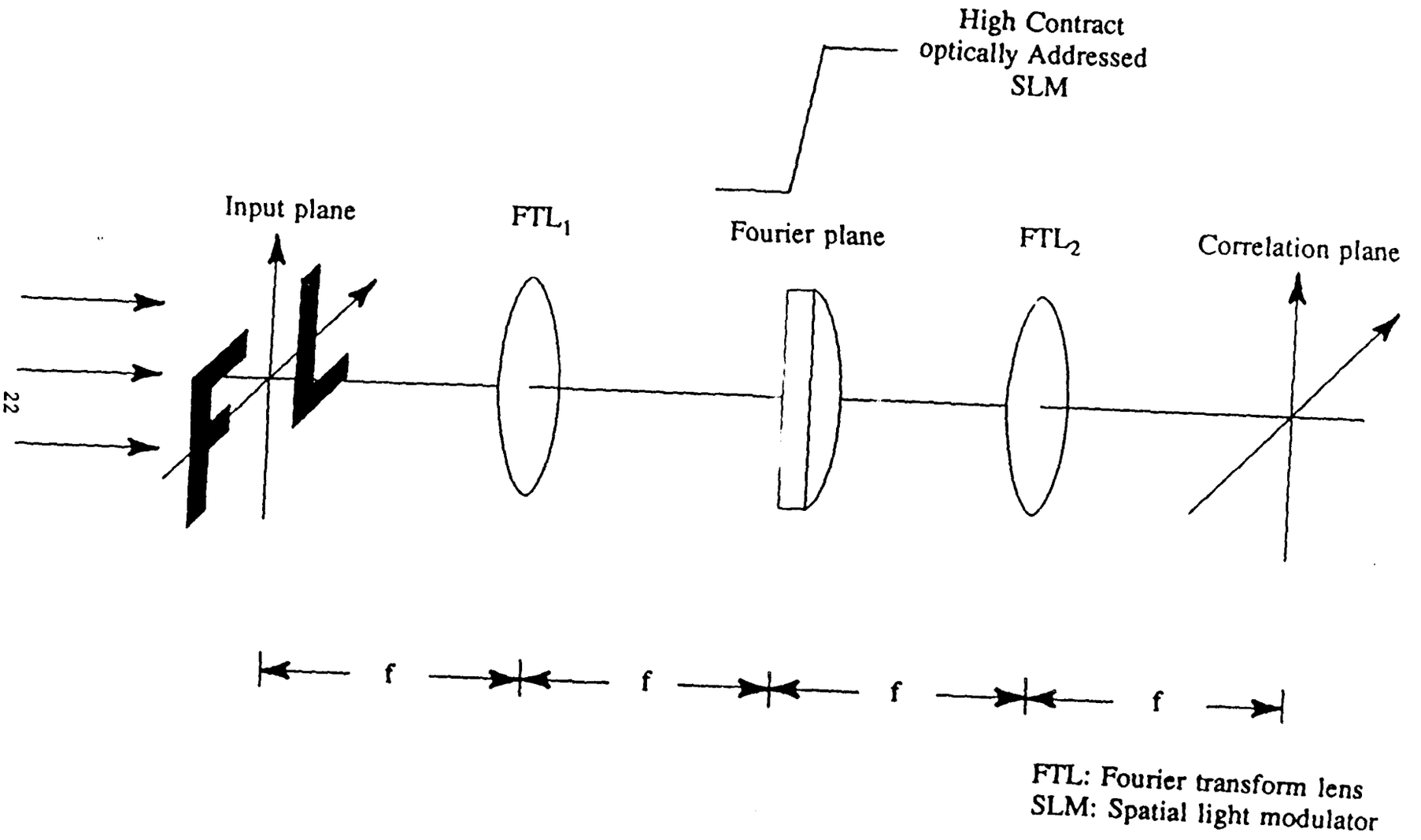

Figure 1 (a) Nonlinear optical correlator implementation using a high contrast optically addressed SLM at the Fourier plane.

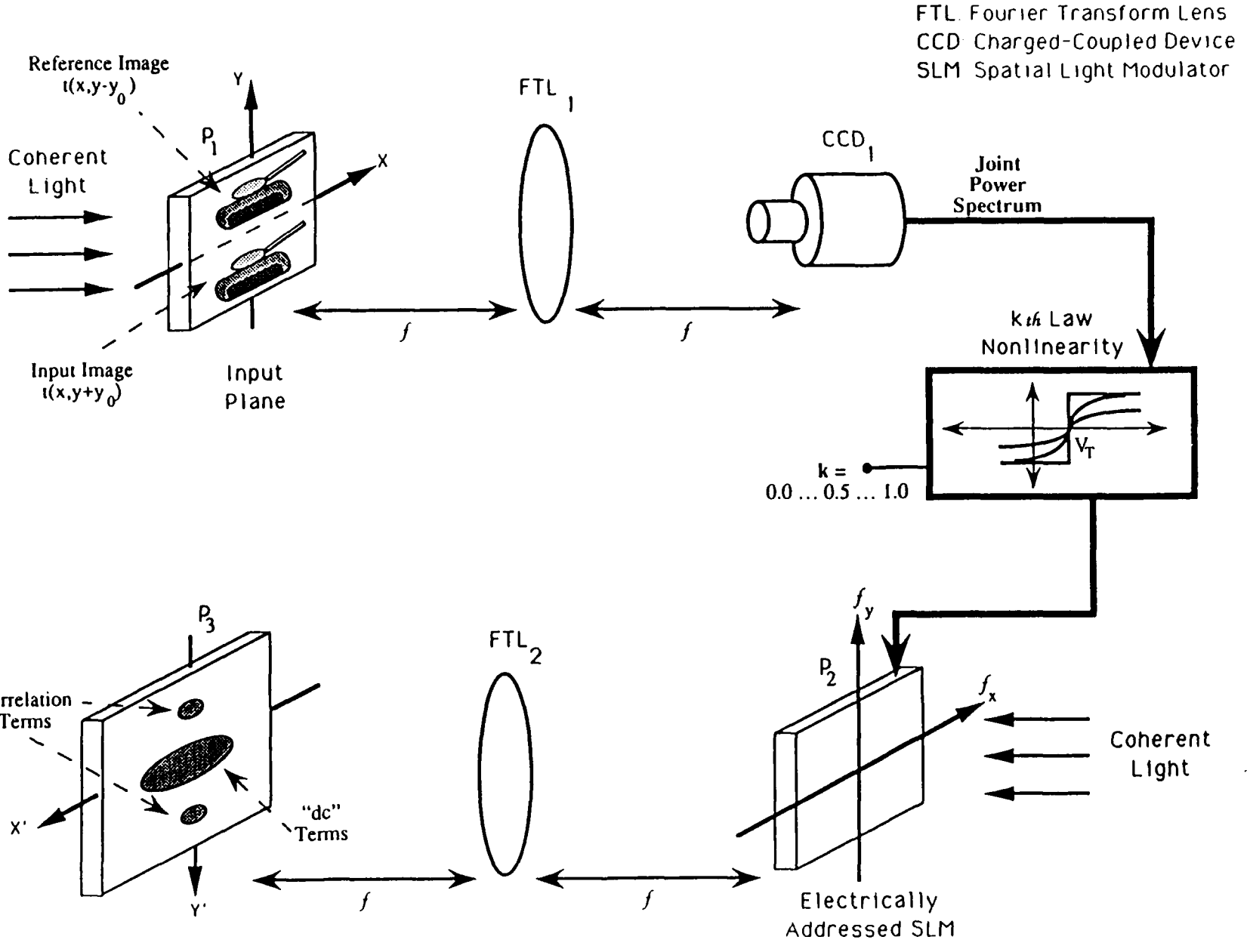
FTL Fourier Transform Lens
CCD Charged-Coupled Device
SLM Spatial Light Modulator
Reference Image
t(x,y-y0)
Coherent
Light
P1
Y
X
Input Image
t(x,y+y0)
Input
Plane
FTL 1
f
f
CCD 1
Joint
Power
Spectrum
kth Law
Nonlinearity
VT
k =
0.0 ... 0.5 ... 1.0
P3
Correlation
Terms
X'
Y'
"dc"
Terms
FTL2
f
f
fy
P2
fx
Coherent
Light
Electrically
Addressed SLM

Figure 1(b)

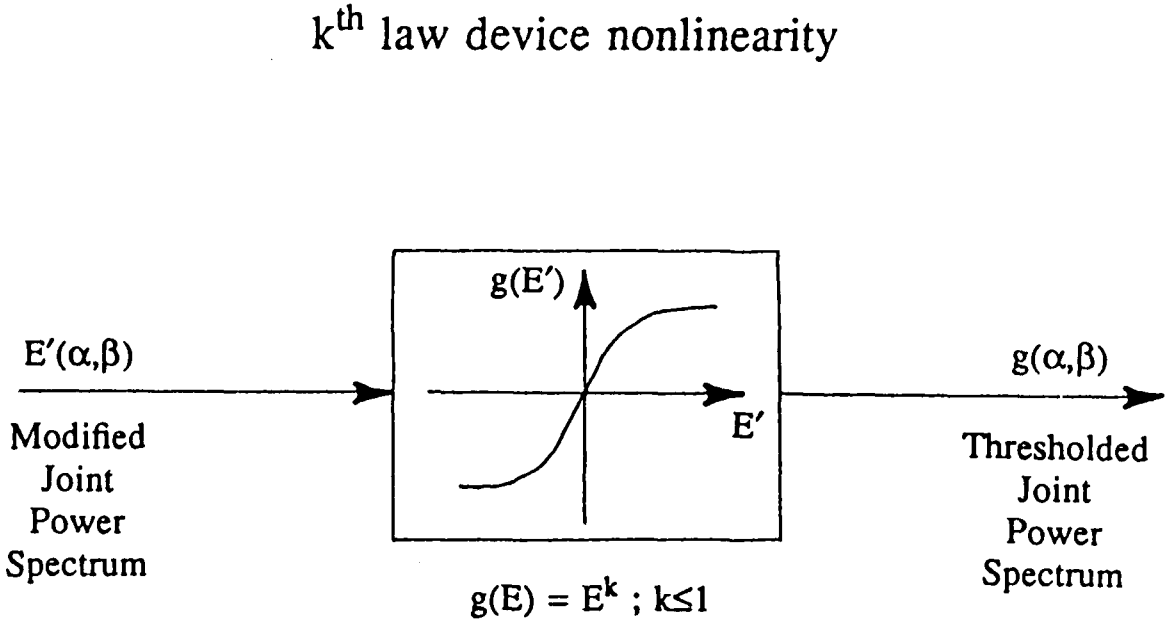

Figure 2. Thresholding network using a k^{th} law device nonlinearity.

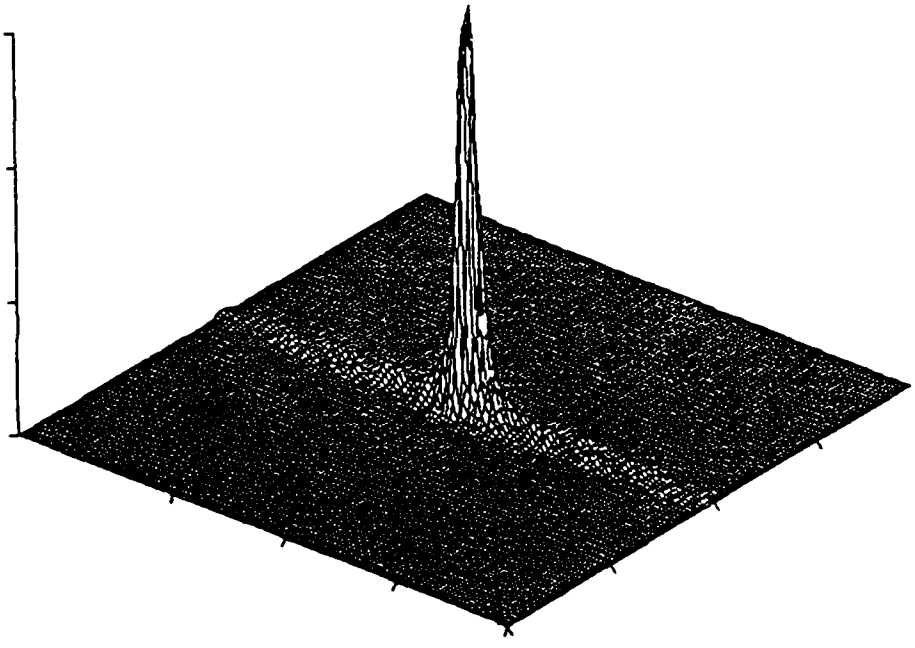

Figure 3 (a) Thresholded modified joint power spectrum using a k^{th} laws device. k=1 corresponds to a linear correlation and the severity of the nonlinearity increases as k decreases.

(a) k=1

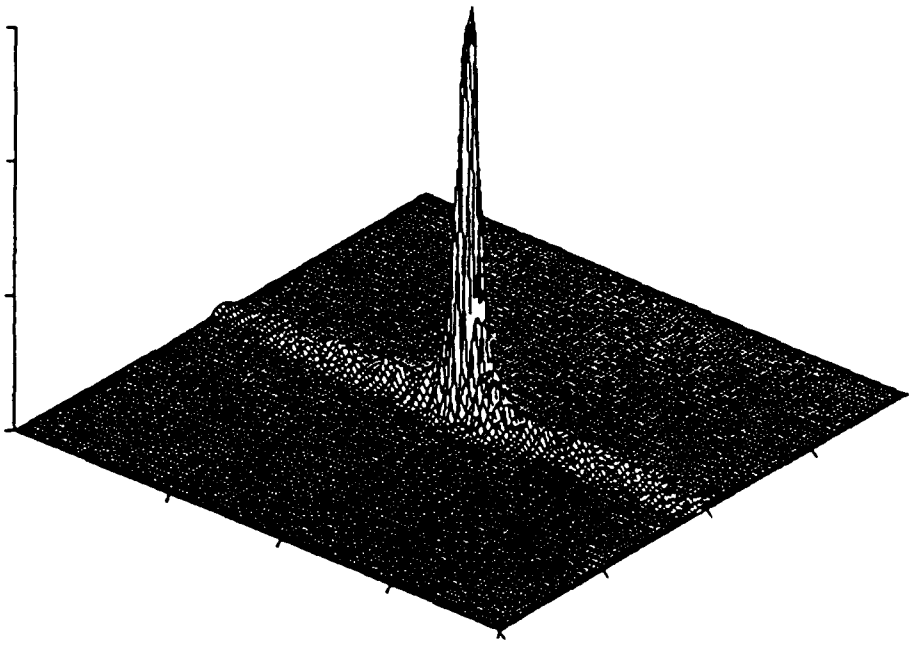

Figure 3 (b) Joint power spectrum for k=0.9.

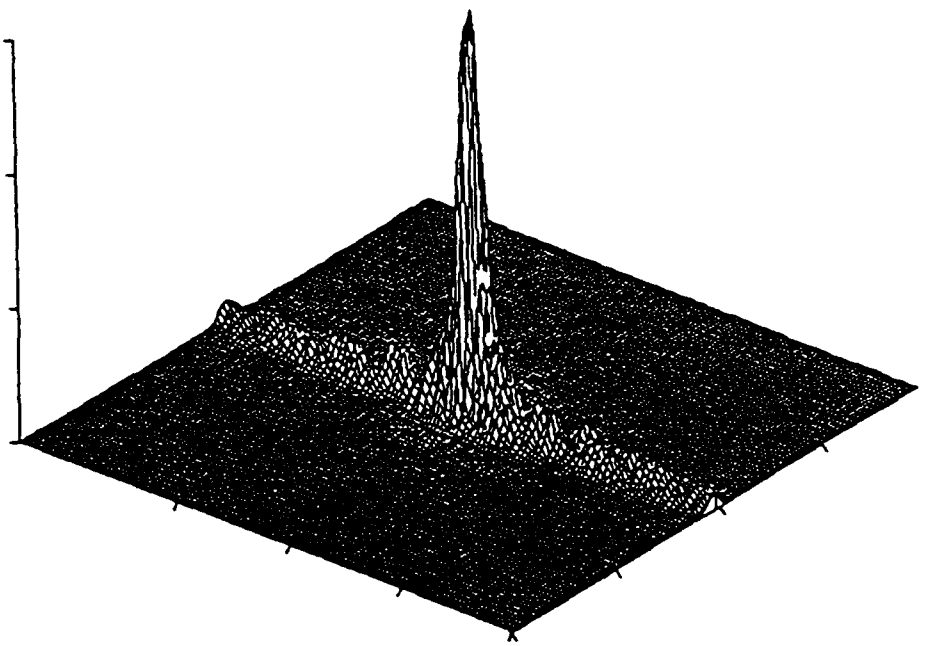

Figure 3 (c) Joint power spectrum for k=0.7.

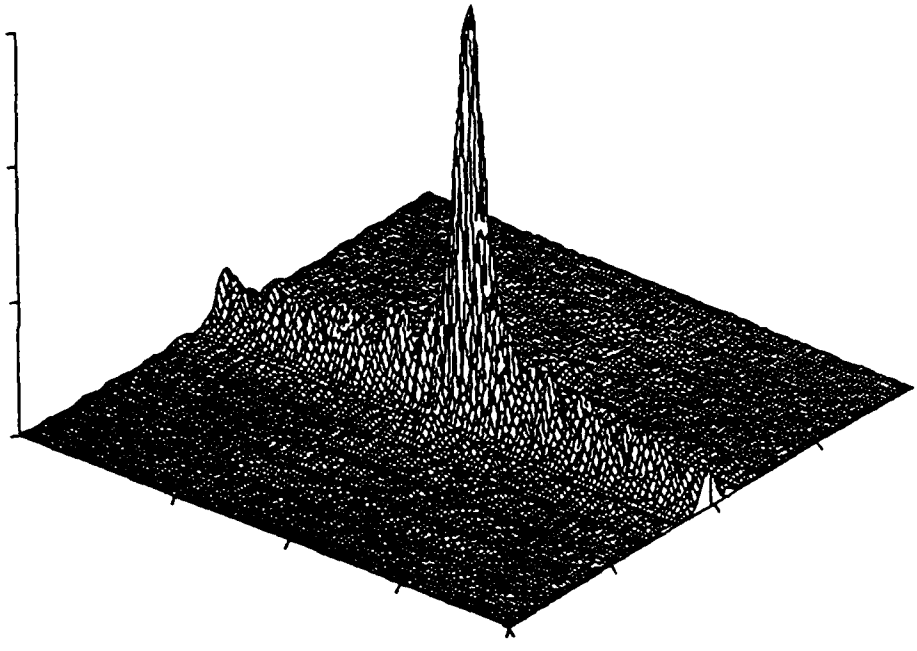

Figure 3(d) Joint power spectrum for k=0.5.

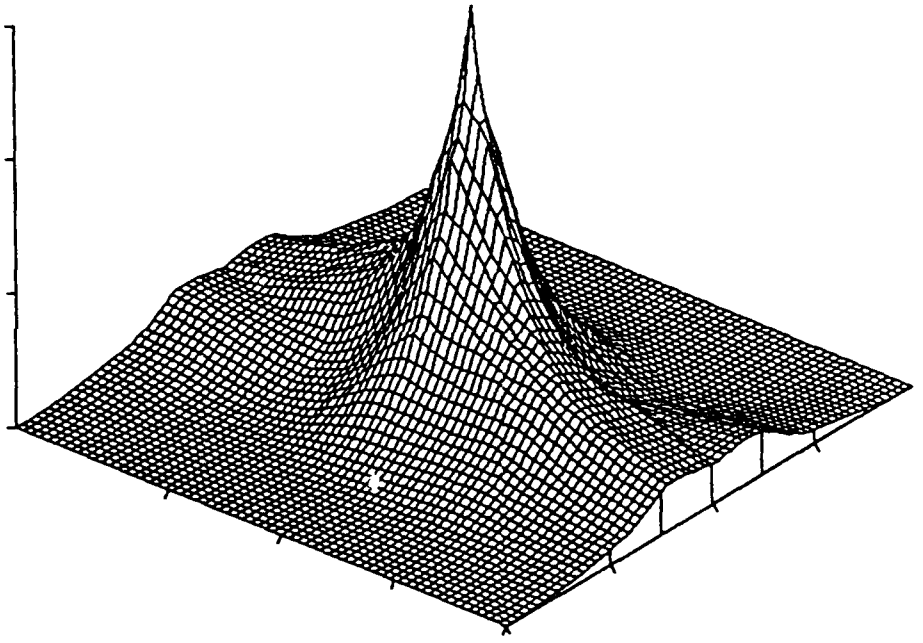

Figure 4. Correlation signals obtained by the thresholded modified joint power spectrum suing a k^{th} law device. k=1 corresponds to a linear correlation and the severity of the nonlinearity increased as k decreases.

(a) k=1

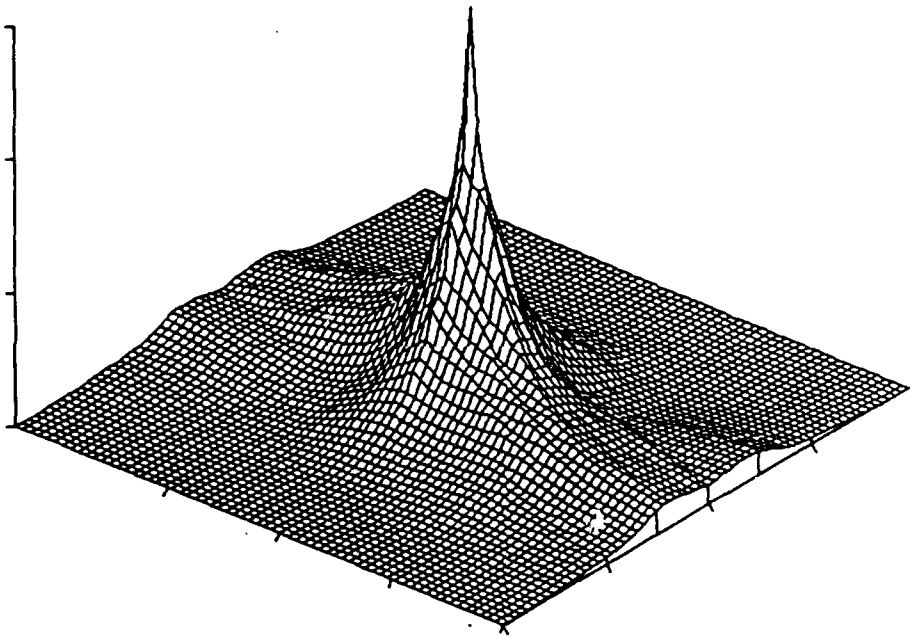

Figure 4.(b) Correlation signals for k=0.9.

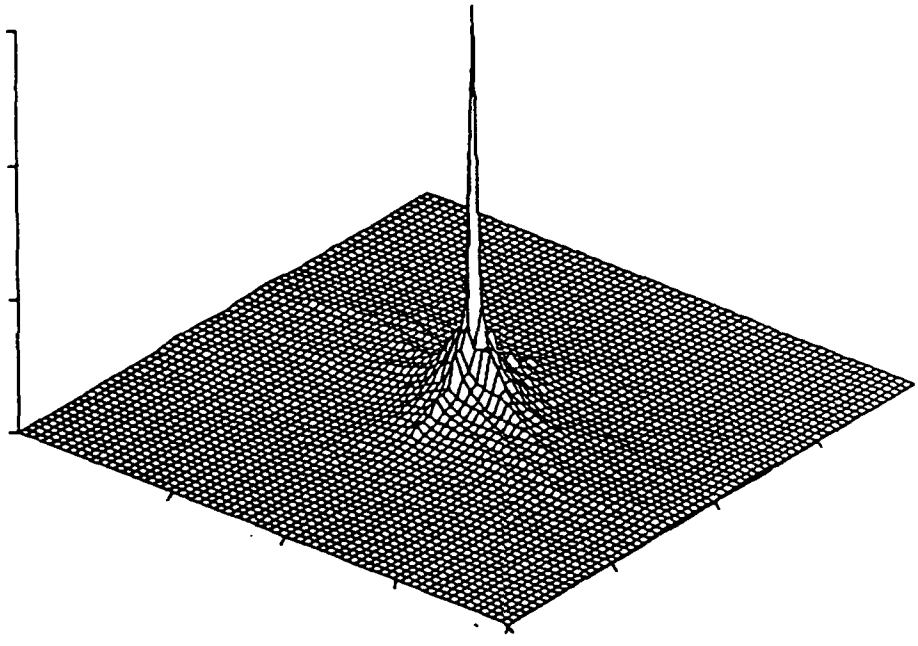

Figure 4 (c) Correlation signals for k=0.7.

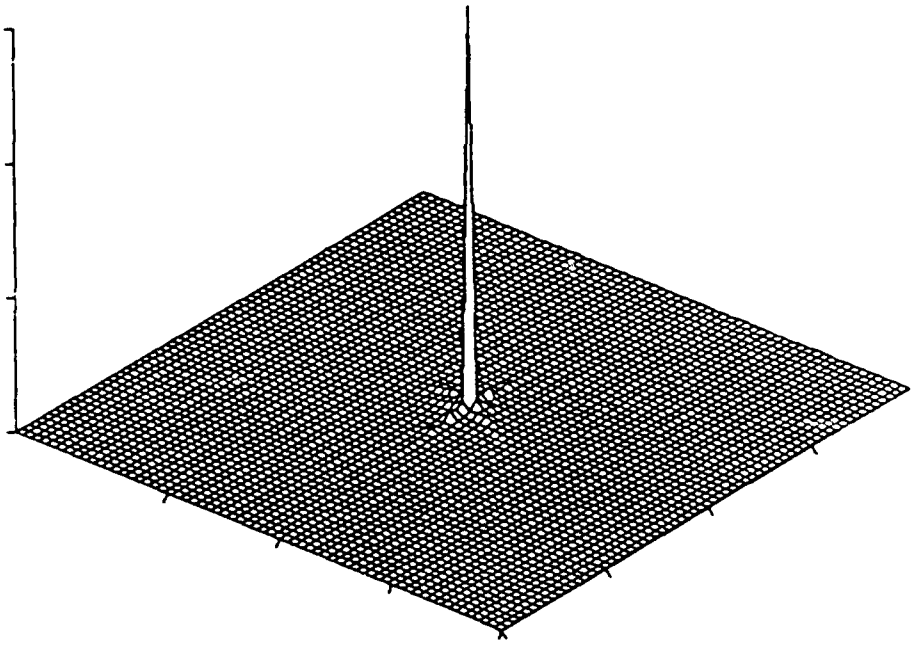

Figure 4 (d) Correlation signals for k=0.5.